

NUMERICAL SIMULATIONS OF FLOW, HEAT TRANSFER AND CONJUGATE HEAT TRANSFER IN THE BACKWARD-FACING STEP GEOMETRY

Federico E. Teruel and Ezequiel Fogliatto

*Grupo de Mecánica Computacional, Centro Atómico Bariloche-CNEA, Bustillo 9500, 8400 San
Carlos de Bariloche, Argentina, teruel@cab.cnea.gov.ar, <http://www.cab.cnea.gov.ar>*

Keywords: Backward-facing step flow, Heat transfer, Conjugate heat transfer, OpenFoam.

Abstract. The objective of this study is to employ the backward-facing step (BFS) flow to verify the implementation of an in-house solver of the incompressible Navier-Stokes equations and energy equation. Additionally, the accuracy and availability of numerical data found in the literature for this problem will be evaluated for fluid flow, heat transfer and conjugate heat transfer cases. For fluid flow, a case with Reynolds number equal to 800 is simulated. Excellent agreement is found with numerical data reported in the literature. For heat and conjugate heat transfer, numerical data is less findable than in the fluid flow case. For heat transfer, present results show differences with available data. Therefore, a heavily tested numerical solver is employed: OpenFoam, as other source of data. Its results agree well with the in-house solver and this suggests that published results may not be fully converged. For conjugate heat transfer a benchmark case is found and is used to be compared with actual simulations. OpenFoam show good agreement with the in-house solver but the benchmark data cannot be well compared. Therefore, further analysis is recommended to find the origin of this disagreement. Data from present simulations for the heat transfer cases is provided in a useful form to be employed for verification and validation purposes.

INTRODUCTION

Fluid flow over a backward-facing step (BFS) is a well known problem extensively used in CFD code verification and validation, especially due to its simple geometry and the presence of interesting phenomena such as flow separation and reattachment. BFS flow characteristics have been extensively studied, for instance, for a variety of Reynolds numbers (Re) (Barton, 1995), step height and expansion ratio (Biswas et al. 2004), and inflow/outflow boundary conditions (Gartling, 1990). In a pioneering study, Armaly et al. (1983) reported measured velocity distribution for laminar flows. This work was extensively employed to validate and verify numerical solutions and to conclude that for Re greater than 400 the flow become three-dimensional yielding different results than those obtained carrying out 2D numerical simulations.

An interesting case analyzed in the nineties for the 2D numerical solution is the BFS flow for $Re = 800$. Gartling (1990) reported a steady and accurate numerical solution of the problem while other studies claim that the laminar solution was not steady for this value of the Re . This controversy was solved by Gresho et al. (1993) who analyzed in detail the numerical stability of this problem concluding that under adequate boundary conditions and adequate spatial and time resolution, the problem is steady. Later, studies like the one carried out by Erturk (2008) reported steady 2D solutions up to $Re = 3000$.

The inclusion of the heat transfer phenomena in the BFS was a natural extension of the fluid flow case. It allows obtaining heat transfer parameters like the Nusselt number (Nu) and to validate and verify numerical implementation of the energy equation in fluid flow solvers. Since many engineering problems involve confined flows with heat transfer, the flow over a BFS with heat transfer and conjugate heat transfer is also a useful benchmark for numerical tools that are aimed to be used with practical purposes. The study of Kondoh et al. (1993) may be cited as a reference of the BFS problem with heat transfer. This study carried out 2D numerical simulations and presents a comprehensive study of the BFS flow for different Reynolds numbers (Re) and expansion ratios, imposing a constant uniform temperature on the bottom channel wall right after the step.

Other step that is useful to validate numerical solvers is to count with data to validate the conjugate heat transfer case. In this direction, there is not easy to find experimental/numerical data for the BFS problem. However, the study of Kanna et al. (2006) intends to present a benchmark case with conjugate heat transfer simulating a finite solid in contact with the bottom wall of the channel, downstream the step. It reported results for a set of Reynolds and Prandtl (Pr) numbers, slab thickness-to-channel thickness ratio and solid-to-fluid thermal conductivity ratio.

The objective of the present study is two fold. First, it is to employ the BFS problem to verify the implementation of an in-house solver of the Navier-Stokes equations and energy equation. And second, to discuss the accuracy and availability of experimental and numerical data of the BFS problem for fluid flow, heat transfer and conjugate heat transfer. These objectives are carried out following several steps. First, the N-S solver is validated employing benchmark data reported by Gartling (1990) for $Re = 800$. This case is a challenge for N-S solvers as the 2D numerical solution tends to be unstable. Additionally, and because the solver is intended to be employed to compute permeabilities, a qualitatively comparison of the N-S solver is presented for the case of Reynolds number going to zero with data provided by Biswas et al. (2004). Next, the energy equation in the flow is tested comparing results with available numerical and analytical data. The analytical solution of an infinite parallel channel

flow with a discontinuity in the wall temperature at origin was analytical solved by [Haji-Sheikh et al. \(2008\)](#), and this solution is employed to test the solver. Moreover, results for heat transfer in the BFS geometry reported by [Kondoh et al. \(1993\)](#) are compared with present results. As results reported by Kondoh appears to be not fully converged, numerical solutions obtained with the open-source tool OpenFoam are included and also compared. Finally, the conjugate heat transfer case reported by [Kanna et al. \(2006\)](#) is compared with present simulations. In this case, there is not agreement and again the open-source code is employed as a third numerical solution to confirm an adequate implementation of the in-house solver. For both, the BFS with heat transfer and conjugate heat transfer, detailed results are reported to be employed as benchmark data.

BACKWARD FACING STEP GEOMETRY AND NUMERICAL METHOD

The BFS flow has the advantages to be described by a simple geometry and to show enough complexity to be considered as a test case. A general representation of the geometry and boundary conditions chosen in this study are shown in [Figure 1](#) for the fluid flow, heat transfer and conjugate heat transfer problems under consideration. Specific boundary conditions, geometrical relationships and parameter definitions will be indicated on each section. The BFS flow features a recirculation region right after the step which length depends on the Reynolds number (see [Figure 1](#)). Additionally, for high enough Re (before transition to turbulence) a second recirculation region appears on the top wall. Moreover, [Erturk \(2008\)](#) obtained laminar and steady solutions up to $Re_H = 3000$ showing several recirculation regions right after the step on both, bottom and top, walls.

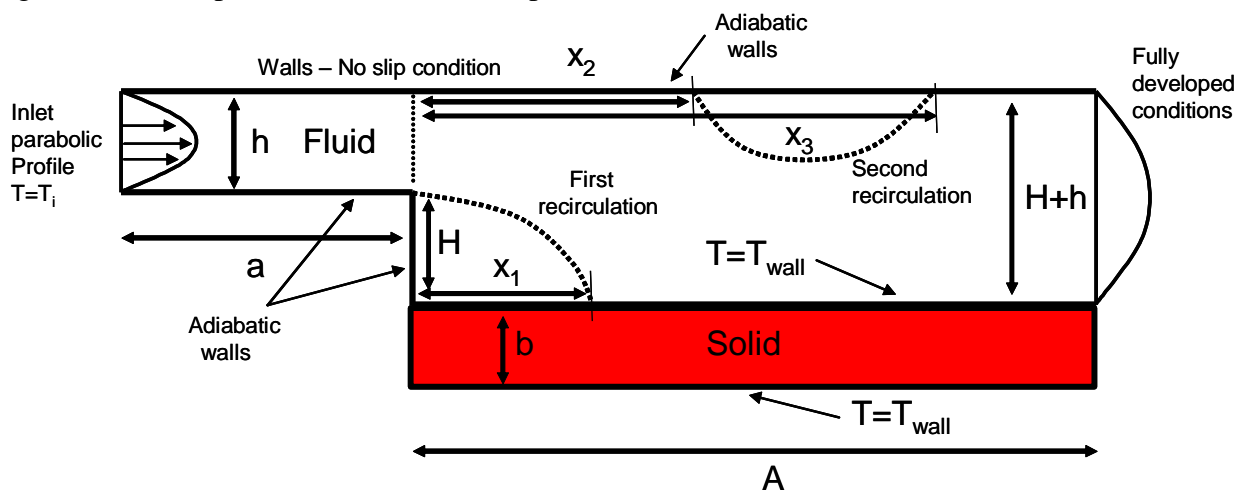


Figure 1: BFS geometry and boundary conditions.

The set of non dimensional equations to be solved in the domain shown in [Figure 1](#) are the incompressible N-S equations and the energy equation respectively:

$$\frac{\partial u_i}{\partial x_i} = 0, \tag{1}$$

$$\frac{\partial u_i}{\partial t} + \frac{\partial}{\partial x_j} u_j u_i = -\frac{\partial p}{\partial x_i} + \frac{1}{Re} \frac{\partial}{\partial x_j} \frac{\partial u_i}{\partial x_j}, \tag{2}$$

$$\frac{\partial T}{\partial t} + \frac{\partial}{\partial x_j} u_j T = \frac{1}{Pe} \frac{\partial}{\partial x_j} \frac{\partial T}{\partial x_j}, \quad (3)$$

where the Peclet number (Pe) is defined as $Pe = Re \cdot Pr$.

In the case of conjugate heat transfer, the energy equation for the solid is added:

$$\frac{\partial T}{\partial t} = k \frac{1}{Pe} \frac{\partial}{\partial x_j} \frac{\partial T}{\partial x_j}, \quad (4)$$

where $k = k_s / k_f$ corresponds to the solid to fluid thermal conductivity ratio. Note that equations have been made non dimensional with the average inlet velocity and the step height.

To solve the set of equations (1-4), the domain was discretized and the finite volume formulation together with the SIMPLER algorithm was employed (Patankar, 1980). To model the diffusion and the convective terms, the central difference and the QUICK scheme were employed, respectively (Leonard, 1979; Hayase et al. 1992). The energy equation is solved at each time step after the velocity and pressure field has been converged. To evolve the initial condition to the steady state a backward Euler scheme was used. Simulations were considered to reach convergence when normalized residuals were lower than 10^{-6} . It has been carefully checked that numerical solutions conserve energy in a global sense (domain); additional details are available in Teruel (2007) and Teruel and Díaz (2013).

As a staggered grid representation was chosen to discretize the problem, boundary conditions are easily to implement and need to be given on the velocity field only for N-S equations. No slip condition was enforced over solid walls and a user-defined velocity profile was set at the inlet (generally, the parabolic profile was imposed). At the outlet, fully developed boundary conditions were employed (Teruel, 2007). For the temperature field, constant wall temperature or constant heat flux was imposed over the volume faces, at boundary walls, for Dirichlet or Neumann boundary conditions respectively.

For the solid-fluid interface (conjugate heat transfer), the continuity in the temperature and heat flux need to be imposed. The recommendation given by Patankar (1980) was followed to compute the heat flux through the interface, where the solution of the 1D problem without sources is assumed, and the harmonic mean is employed to compute an equivalent thermal conductivity at the solid-fluid interface.

The domain was discretized, depending on the case, using a uniform and structured grid of squares or a non uniform grid that is refined near walls according the procedure described in Teruel(2007).

When the open-source code was employed to compare results with the in-house solver, the discretization, boundary conditions and parameter definitions were the same, or equivalent, to those used in the simulations carried out with the in-house solver.

FLUID FLOW VERIFICATION

The locations of the separation point X_2 , and the reattaching points X_1 and X_3 as a function of the Re is very well studied and is going to be used to verify the code (see Figure 1). Additionally, velocity and pressure profiles reported in literature are going to be compared with present results. Note that the energy equation is not solved in this section.

The 2D BFS flow for $Re_{2H} = 800$ (based on average inlet velocity) has been studied in detail. Gartling (1990) carried out a highly resolved numerical simulation of this problem reporting profiles of relevant variables at different locations after the step. Further on, in early

nineties, discussions aroused regarding the steadiness of the 2D numerical solution of this problem. Different authors reported time dependant solutions or solutions that were unstable under small perturbations. Gresho et al. (1993) carried out an exhaustive study concluding that the solution is steady and stable. In cases presented here, solutions reached a steady-state. Results for $Re_{2H} = 800$ are presented in Table 1 for different uniform grid resolutions. Domain was extended from the step ($a = 0$) to $31H$ using an uniform grid and continuing with a geometric-grid (see Teruel, 2007) up to $A = 45H$ to save computational time. For this case $H = h$ and a parabolic velocity profile is imposed right at the step. Note that for this Re the flow is three-dimensional and for that reason, 2D numerical data do not agree with experimental results.

| Control Volumes per step height (H) | X_1/H | X_2/H | X_3/H |
|-------------------------------------|-----------|---------|---------|
| 10 | 11.0 | 9.0 | 19.7 |
| 20 | 11.9 | 9.6 | 20.5 |
| 30 | 12.1 | 9.7 | 20.7 |
| 44 | 12.2 | 9.8 | 20.8 |
| 64 | 12.2 | 9.8 | 20.9 |
| Gartling (1990) | 12.20 | 9.70 | 20.96 |
| Barkley et al. (2002) | 11.9 | 9.5 | 20.6 |
| Williams and Baker (1997) | 11.4-12.2 | - | - |

Table 1: Reattachment and separation points of the laminar BFS for $Re_{2H} = 800$ and different grid resolutions.

A more detailed comparison of the numerical results obtained for $Re_{2H} = 800$ is carried out in the following figures. Gartling reported relevant numerical values at two different locations measured from the step: 14 and 30 x/H respectively. Figure 2 shows cross sections for the streamwise and vertical velocities as well as for pressure and vorticity at these locations. The correct profile of the vertical velocity component at $x/H = 14$ is difficult to capture. Different grid solutions are presented for this quantity to show that this flow requires a high resolution to be represented correctly. Other quantities plotted in Figure 2 correspond to the solution found with the finer grid solution (i.e. uniform grid, 64 control volumes (CVs) per step height). The agreement shown between 2D numerical simulations of the BFS and results calculated here is excellent regarding the location of reattachment/separation points and also with profiles of velocities and pressure across and along the channel.

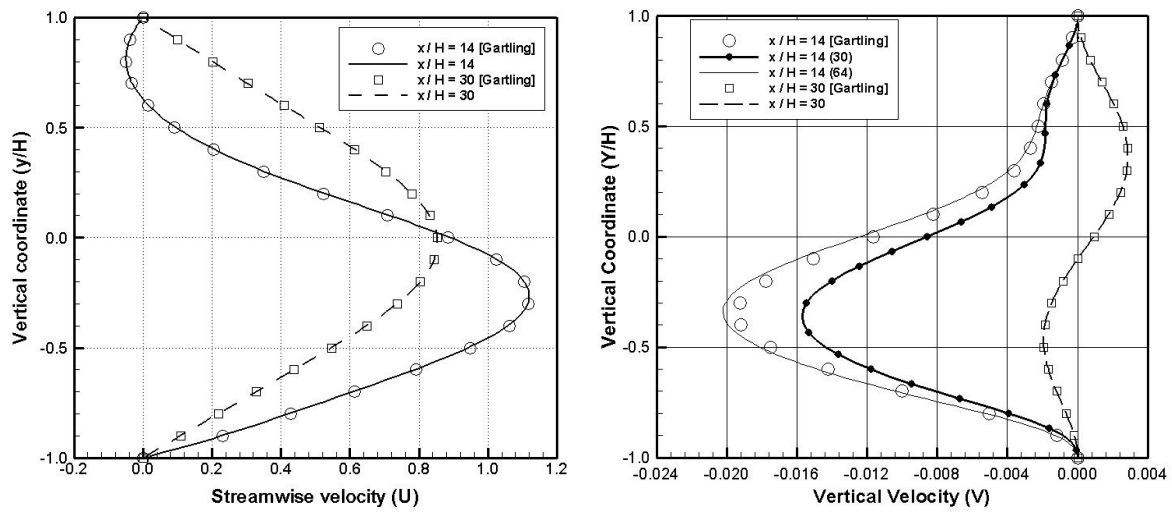


Figure 2a: Streamwise and vertical velocities. Right panel: 30 and 64 indicates the control volumes per step height (uniform grid).

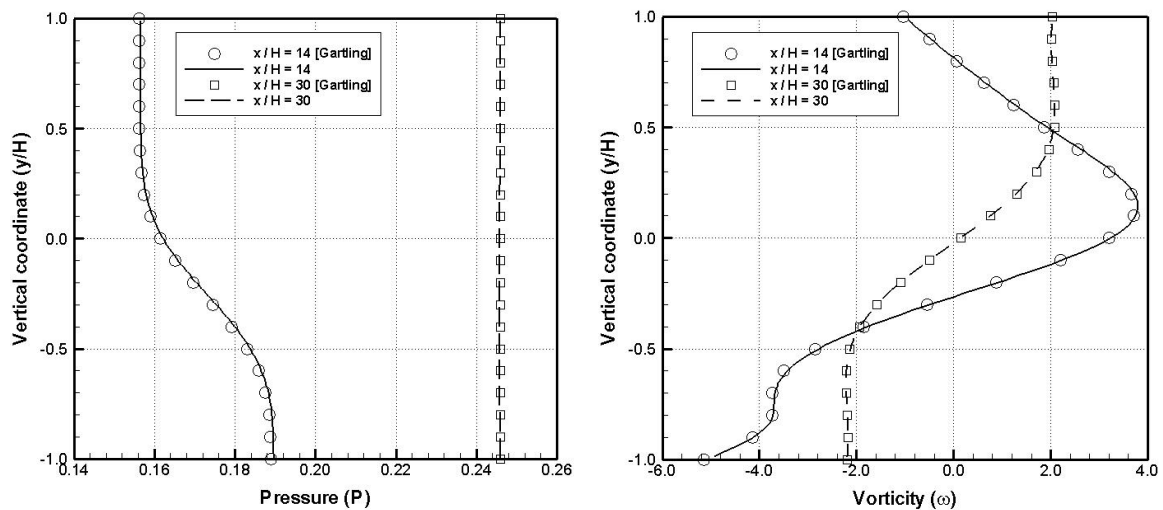


Figure 2b: Pressure and vorticity.

Figure 2: Profile comparison at $x/H = 14$ and 30 respectively. Laminar BFS for $Re_{2H} = 800$. Values reported by Gartling and present results.

The order of accuracy of the N-S solver coded in this work can be study considering for instance, the reattachment/separation locations as a function of the grid size. This aspect is important to test the convergence of the numerical solution and to detect erroneous implementations of the solver. The order of accuracy can be estimated considering the error respect to a fine grid calculation as a function of the grid spacing. Figure 3 shows the errors in X_1 , X_2 and X_3 respect to values calculated here with the finer grid (64 CVs step height). Based on Figure 3, it is fair to say that the solver converge with approximately a second order accuracy in the case of uniform grid spacing as it is expected according to the numerical schemes used.

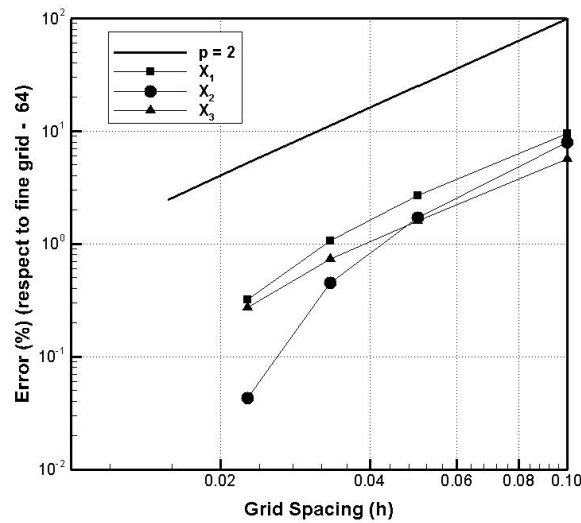


Figure 3: Convergence as a function of the grid spacing for the location of X_1 , X_2 and X_3 .

The in-house solver is intended to be employed to calculate porous media flow and heat transfer. One of the relevant parameters to describe porous media flows is the permeability. Although Stokes's flow type simulations are pertinent to compute this parameter, it can also be carried out solving the complete N-S equations for low Re and extrapolating results to the limit of zero Re (e.g. [Martin et al. \(1998\)](#); [Edwards et al. \(1990\)](#)). To evaluate the performance of the N-S solver implemented here when calculating low Re flows, the BFS geometry was considered. The same boundary conditions as those employed for the $Re_{2H} = 800$ case were employed. The domain is set with $H = h$. In the streamwise direction it is extended from $a/H = 1$ to $A/H = 3$. Re_H numbers equal to 10^{-4} , 10^{-2} and 1 were simulated (based on average inlet velocity). [Biswas et al. \(2004\)](#) reported numerical results for this geometry and low Re capturing two Moffatt eddies ([Moffatt, 1964](#)) at the lower corner of the step (note that slightly different from the geometry simulated here, [Biswas et al. \(2004\)](#) employed a step height of $0.9423h$). According to Biswas, the sizes of the first and second eddies ($Re_H = 1$) are approximately 0.4 and 0.02 (over the vertical wall, normalized with the step height). It is of interest then to compute a resolved simulation to capture these two eddies when. For this purpose, the domain was partitioned with a non uniform grid in the square defined by the vertical wall of the step (150×150 elements) and the rest of the domain was partitioned using 64 elements per step height. The resolution in the lower corner of the step was 10^{-3} step units, yielding 20×20 CVs to resolve the second eddy. Results obtained here are very well compared with those reported by Biswas ([Figure 4](#), streamlines).

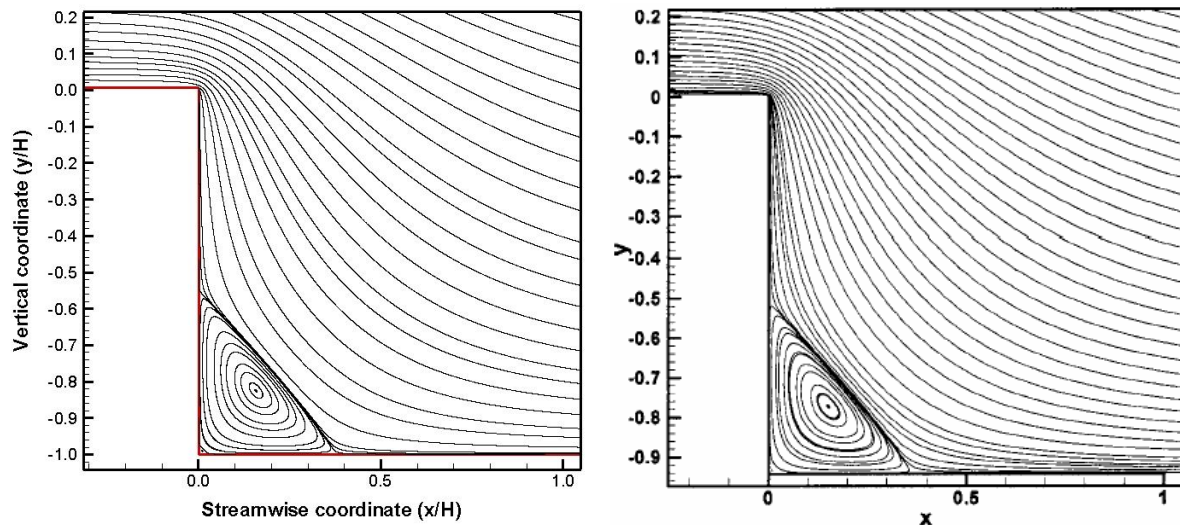


Figure 4a: Streamlines after the step. First Moffatt vortex shown.

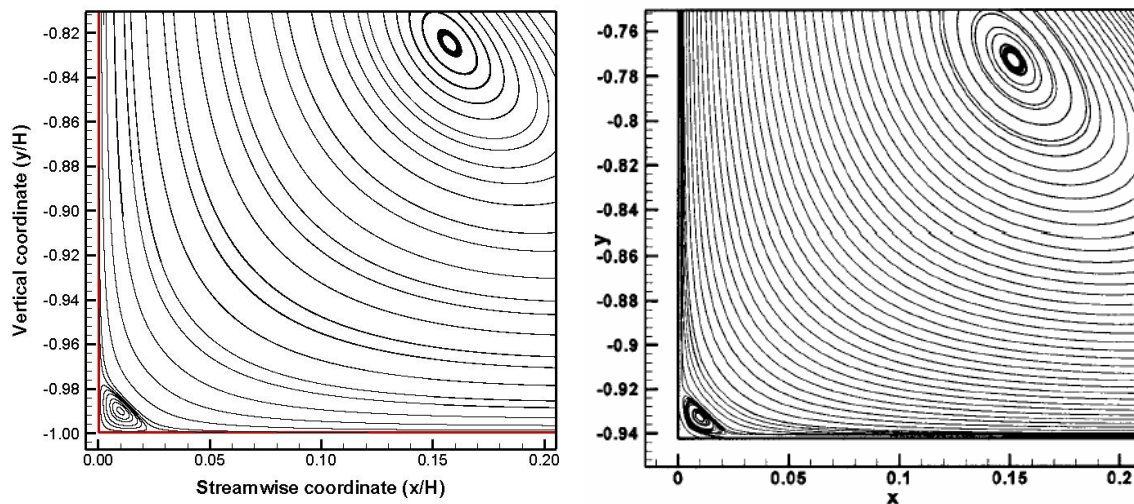


Figure 4b: Zoom near the bottom corner. Center of first vortex and second vortex shown.

Figure 4: Visual comparison of the streamlines of the flow between present results (left) and those reported by Biswas (right). First and second Moffatt eddies are captured by the numerical simulation.

THERMAL FIELD VERIFICATION

The implementation of the transport equation for a passive scalar (i.e. temperature in this case), is first verified by comparison with analytical results. [Haji-Sheikh et al. \(2008\)](#) recently reported a power series analytical solution for an infinite parallel channel flow with a parabolic velocity profile, that presents a step change in the wall temperature at the center of the channel ($x = 0$). This problem is adequate for the present verification as the solution is strongly dependent on the Pe and allows testing the energy equation isolated from the momentum equation. Although the analytical solution was obtained in an infinite domain, the domain shown in [Figure 5](#) has been tested to be sufficient for the Pe number simulated. Note that zero heat flux is imposed on the inlet-outlet boundaries of the domain.

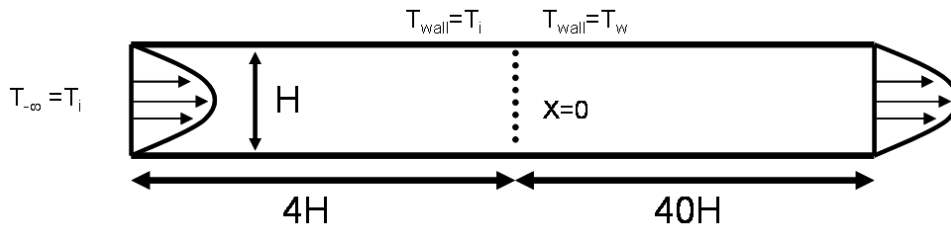


Figure 5: Domain employed in the numerical simulation of the Haji-Sheikh' problem.

Figure 6 (left panel) shows the non dimensional bulk temperature ($\theta_b = (T_b - T_{wall}) / (T_{in} - T_{wall})$) for $x > 0$ for different Pe in the 1-10 range. The comparison between the code and the analytical solution is excellent. A similar trend is shown for the fully developed Nu faraway from the origin and considering a larger range for the Pe than in the left panel. This case, although useful to verify several aspects in the implementation of the energy equation, fail to test the transport of the scalar in the vertical direction by convection as the velocity is only one dimensional. Therefore the BFS problem is recalled.

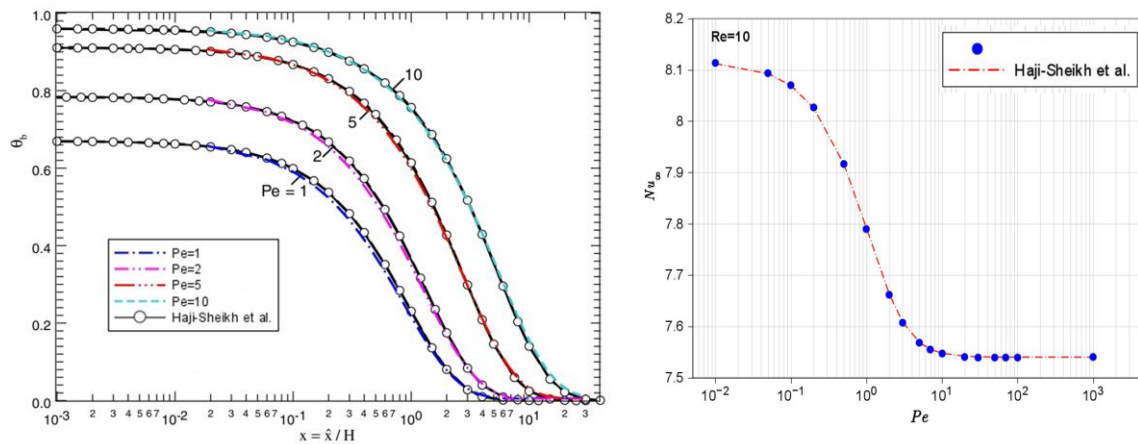


Figure 6: Temperature (left) and Nusselt number (right) for different Pe numbers.

Unfortunately, the Authors do not have knowledge of benchmark numerical results for the heat transfer problem in the BFS. Nevertheless, in an often cited study, [Kondoh et al. \(1993\)](#) reported results for this geometry and with a wall temperature in the lower wall downstream the step different from that at the inlet (see [Figure 1](#)). Different Re , Pe and expansion ratios are numerically simulated and presented in plot forms. Two cases are considered here for verification purposes. In both, the geometry is defined as $h = 2H$, $a/H = 5$, $A/H = 40$ and a parabolic profile is imposed at the inlet. In the first case the following values are simulated: $Re_H = 100$ and $Pe = 71$. The parameter of interest is the local Nu calculated at the bottom wall downstream the step. As results reported by Kondoh do not accurately match present results, a third set of results obtained with OpenFoam are presented (see [Figure 7, left](#)). Present simulations agree very well. This difference may be originated in the nowadays poor resolution employed in Kondoh' study (120×60 against 1800×60 , streamwise x vertical directions). To validate this hypothesis, data from Lewis et al. (2004) is compared for this case and for different Re ([Figure 7, right](#)). The agreement is excellent for all Re simulated. Note that the $Pr = 0.71$ for these simulations.

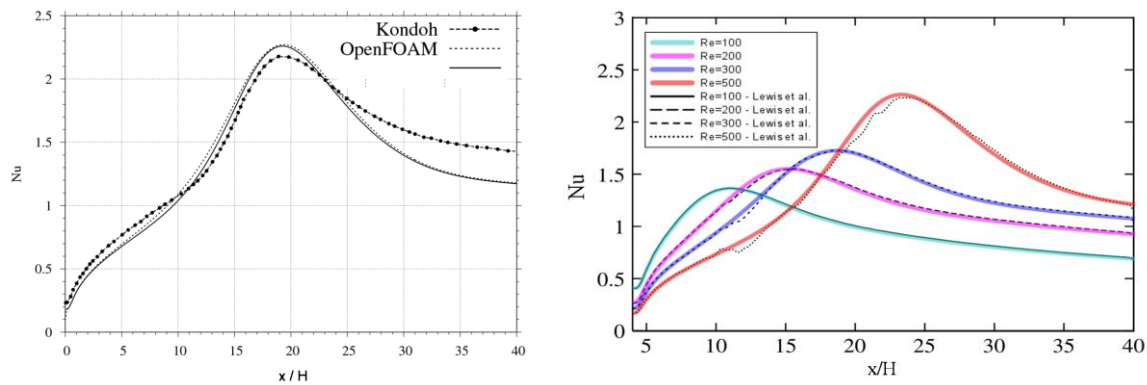


Figure 7: Nusselt number for the BFS flow. Comparison with Kondoh (left) and Lewis (right).

This problem becomes more challenging if both the Re and Pe are increased. The case for $Re_H = 500$ and $Pe = 3500$ is presented in Figure 8 for a variety of parameters and with the same geometry as that employed for data shown in Figure 7. The in-house code is used with uniform grids and non uniform grids with refinement at walls. Kondoh's results are also included for comparison purposes and do not agree well with the more accurate results computed here (this study employed a non uniform grid of 120×60 CVs). In this case, the advection of the passive scalar dominates yielding sharp gradients that require a fine discretization to avoid errors in the calculation of the Nu . Note that the Nusselt number peak changes in a 7% value when the grid is refined from 36 to 72 CVs per step height. It is interesting to point out that for this particular simulation the solution converge from "below" and from "above" for non uniform and uniform grids respectively. This allows narrowing the maximum Nu between 4.59 and 4.73 for present simulations. It is important to note that a non uniform grid allows capturing the converged solutions with considerable less grid points than in the uniform case despite the fact that the convergence order is theoretically lower for this type of grids than for uniform ones.

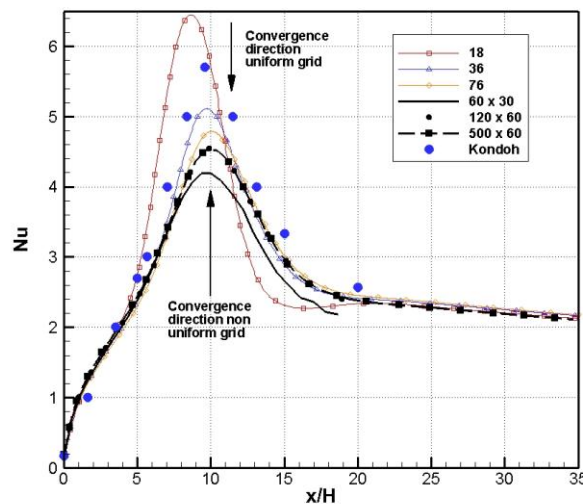


Figure 8: Nusselt number for the BFS flow. $Re_H = 500$ and $Pe = 3500$. Different grid resolutions for uniform and non uniform grids. Also Kondoh's results for comparison.

Table 2 shows local values of the local Nusselt number along the bottom wall and cross sections of the temperature field at two different locations: $x/H = 5$ and 7 . Note that these results were obtained with the maximum grid resolution for uniform grids. These values are considered more accurate than those reported in Kondoh et al. (1993) and may be employed for verification purposes.

| x/H | Nu | y/H | θ (x/H=0.51) | θ (x/H=2.51) | θ (x/H=5.01) | θ (x/H=8.01) |
|-------|------|-------|---------------------|---------------------|---------------------|---------------------|
| 0.01 | 0.30 | -0.49 | 0.98 | 0.96 | 0.95 | 0.91 |
| 2.01 | 1.61 | -0.41 | 0.84 | 0.68 | 0.54 | 0.32 |
| 4.01 | 2.27 | -0.32 | 0.72 | 0.48 | 0.34 | 0.21 |
| 6.01 | 3.09 | -0.24 | 0.63 | 0.40 | 0.33 | 0.18 |
| 8.01 | 4.49 | -0.16 | 0.58 | 0.41 | 0.35 | 0.11 |
| 9.01 | 5.19 | -0.07 | 0.60 | 0.45 | 0.26 | 0.03 |
| 10.01 | 5.42 | 0.01 | 0.39 | 0.22 | 0.07 | 0.00 |
| 11.01 | 5.10 | 0.09 | 0.00 | 0.01 | 0.00 | 0.00 |
| 13.01 | 3.93 | | | | | |
| 17.01 | 2.74 | | | | | |
| 21.01 | 2.50 | | | | | |
| 25.01 | 2.41 | | | | | |

Table 2: Nu and non dimensional temperature for Kondoh' geometry. $Re_H = 500$, $Pe = 3500$ and uniform grid (72 CVs per step height)

CONJUGATE HEAT TRANSFER VERIFICATION

To model conjugate heat transfer, the energy equation on the solid phase is added, and the continuity of temperature and heat flux is imposed at the solid-fluid interface. Recently, [Kanna and Das \(2006\)](#) studied the conjugate BFS with a finite solid in contact with the bottom wall of the channel, downstream the step. They reported results for a set of Re and Pe , slab thickness and solid-to-fluid thermal conductivity ratio in a benchmark fashion (i.e. numerical simulations are well described and numerical results are reported in table form at different locations). In this section, the open-source tool and the in-house solver are employed to make a revision of this published result. The Authors are not aware of other set of data ready to be used for verification purposes.

Results by [Kanna and Das \(2006\)](#) do not agree well with present simulations. [Figure 9](#) shows results for the following geometry: $h=H$, $a/H = 0$, $b/H = 1$, $A/H = 60$, and following parameters: $Re_H = 500$, $k = 2$ and $Pe = 50$ and 355 . While OpenFoam and the in house code agree very well on the Nu number (left panel) and temperature at the interface (right panel), they strongly differ from benchmark results. Unfortunately, Kanna and Das do not verify their code for the case of conjugate heat transfer and the paper has not been cited by studies that analyze these results. In one hand, Authors recognize that present results require further verification to clarify the reason of the difference reported here (note that experimental results may differ from numerical simulations as the flow is three-dimensional for this Re and other independent numerical results will be welcomed). On the other hand, as the in-house solver reproduces very well the data obtained with OpenFoam, it is speculated that the conjugate solver has been correctly implemented. For further verification, results for cases presented in [Figure 9](#) are shown in table form (see [Table 3](#)).

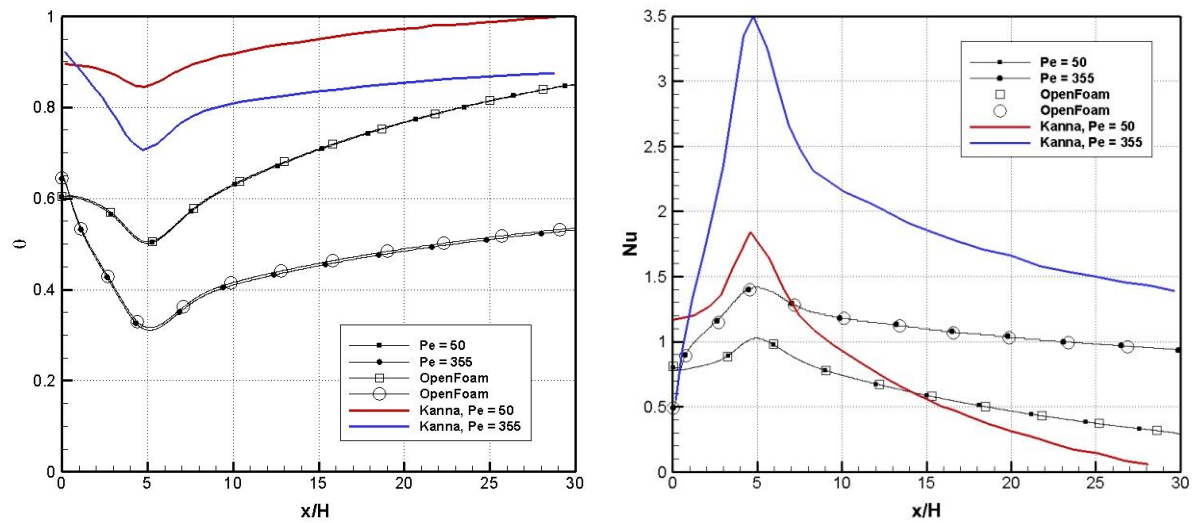


Figure 9: Nusselt number for the BFS conjugate heat transfer. $Re_H = 500$ and $k = 2$.

| x/H | Nu | y/H | θ (x/H=0.25) | θ (x/H=1.5) |
|-------|------|-------|---------------------|--------------------|
| 0.02 | 0.60 | -2.55 | 0.91 | 0.90 |
| 2.02 | 0.69 | -2.05 | 0.81 | 0.80 |
| 4.02 | 0.80 | -1.55 | 0.72 | 0.69 |
| 6.02 | 0.90 | -1.15 | 0.66 | 0.61 |
| 8.02 | 0.98 | -1.05 | 0.65 | 0.59 |
| 10.02 | 1.02 | -0.95 | 0.63 | 0.56 |
| 12.02 | 1.01 | -0.75 | 0.58 | 0.48 |
| 14.02 | 0.97 | -0.55 | 0.54 | 0.42 |
| 16.02 | 0.93 | -0.35 | 0.49 | 0.36 |
| 20.02 | 0.89 | -0.15 | 0.40 | 0.29 |
| 23.02 | 0.86 | 0.05 | 0.09 | 0.12 |
| 26.02 | 0.85 | 0.25 | 0.00 | 0.01 |
| 29.02 | 0.83 | 0.45 | 0.00 | 0.00 |
| 32.02 | 0.81 | | | |

Table 3: Nu and non dimensional temperature for Kanna' geometry. $Re_H = 500$, $Pe = 355$ and uniform grid (60 CVs per step height).

SUMMARY AND CONCLUSIONS

In this study, an in-house N-S equations and energy equation solver was tested employing numerical results for the BFS flow. The open-source code OpenFoam was also employed as a second independent numerical source of data in cases where published data differs from that obtained in present simulations. First, the fluid flow solver was verified for the BFS configuration simulated by Gartling (1993). Present results showed an excellent comparison with published data for this numerically demanding (i.e. dominated by advection effects) laminar flow. Additionally, a qualitative comparison was carried out for the BFS in the limit of zero Re . In this case, an infinite set of Moffatt vortices appears, and the code was shown to be able to capture them when the grid is appropriately defined. Thermal field calculations are more difficult to be accurately compared as results are not as rich as in the flow case. A

simple but strong Pe dependant case of a laminar channel flow was the first step to account for a correct implementation of the energy equation solver. Later, the thermal field in the BFS flow was compared with results published by Kondoh et al. (1993). There is not a complete agreement for moderate Pe though the in-house solver agrees very well with OpenFoam. The comparison for large Pe with present results as a function of the grid size seems to imply that Kondoh et al. results are not fully converged. Finally, the literature provides a benchmark case for the conjugate heat transfer problem. Present results, although in good agreement with the second source of numerical data, completely disagree with the benchmark. Unfortunately, there is a not paper that have agreed or discussed data reported in the benchmark.

The BFS flow has been found to be an excellent case of study to test and validate numerical results. The geometry is easy to implement as well as boundary conditions. Accurate numerical data in table form is however needed for heat and conjugate heat transfer cases. This study provides a set of numerical data extracted from the simulations that can be employed by other Authors for verification purposes. The in-house solver has been proved to deliver accurate results that give confidence to simulate flows other than the BFS.

REFERENCES

- Armaly, B.F., Durst, F., Pereira, J.C.F. and Schönung, B., Experimental and theoretical investigation of backward-facing step. *Journal of Fluid Mechanics*, 127:473-496, 1983.
- Barkley, D., Gomez, M.G.M., and Henderson, R.D., Three-dimensional instability on flow over a backward-facing step. *Journal of Fluid Mechanics*, 473:167-190, 2002.
- Barton, I.E., A numerical study of flow over a confined backward-facing step. *International Journal for Numerical Methods in Fluid*, 21:653-665, 1995.
- Biswas, G., Breuer, M. and Durst, F. Backward-facing step flows for various expansion ratios at low and moderate Reynolds numbers. *Journal of Fluids Engineering*, 126:62-374, 2004.
- Edwards, D.A., Shapiro, M., Bar-Yoseph, P. and Shapira, M., The influence of Reynolds number upon the apparent permeability of spatially periodic arrays of cylinders. *Physics of Fluids A*, 2:45-55, 1990.
- Erturk, E., Numerical solutions of 2-d steady in-compressible flow over a backward-facing step, Part I: High Reynolds number solutions. *Computer and Fluids*, 37:633-655, 2008.
- Gartling, D.K., A test problem for outflow boundary conditions—flow over a backward-facing step. *International Journal for Numerical Methods in Fluids*, 11:953-967, 1990.
- Gresho, P.M., Gartling, D.K., Torczynski, J.R., Cliffe, K.A., Winters, K.H., Garratt, T.J., Spence, A. and Goodrich, J.W. Is the steady viscous incompressible two-dimensional flow over a backward-facing step at $Re = 800$ stable? *International Journal for Numerical Methods in Fluids*, 17:501-541, 1993.
- Haji-Sheikh, A., Beck, J.V. and Amos, D.E., Axial heat conduction effects in the entrance region of parallel plate ducts. *International Journal of Heat and Mass Transfer*, 51:5811-5822, 2008.
- Hayase, T., Humphrey, J.A.C. and Greif, R., A Consistently formulated QUICK scheme for fast and stable convergence using finite-volume iterative calculation procedures. *Journal of Computational Physics*, 98:108-118, 1982.
- Kanna, P. and Das, M., Conjugate Heat Transfer Study of Backward-Facing Step Flow. *International Journal of Heat and Mass Transfer*, 49:3929-3941, 2006.
- Kondoh, T., Nagano, Y. and Tsuji, T., Computational study of laminar heat transfer downstream of a backward-facing step. *International Journal of Heat and Mass Transfer*, 36:577-591, 1993.

- Leonard, B.P., A stable and accurate convective modeling procedure based on quadratic upstream interpolation. *Computer Methods in Applied Mechanics Engineering*, 19:59-98, 1979.
- Lewis, R.W., Nithiarasu, P. and Seetharamu, K.N., *Fundamentals of the finite element method for heat and fluid flow*, John Wiley & Sons, Ltd, 2004.
- Martin, A.R., Saltiel, C. and Shyy, W., Friction losses and convective heat transfer in sparse, periodic cylinder arrays in cross flow. *International Journal of Heat and Mass Transfer*, 41:2383-2397, 1998.
- Moffatt, H.K., Viscous and resistive eddies near a sharp corner. *Journal of Fluid Mechanics*, 18:1-18, 1964.
- Patankar, S.V. *Numerical Heat Transfer and Fluid Flow*, Hemisphere, 1980.
- Teruel, F.E., 2007. *Macroscopic Turbulence Modelling and Simulation for Flow Through Porous Media*. PhD Thesis, University of Illinois at Urbana-Champaign, USA, 2007.
- Teruel, F.E. and Díaz, L., Calculation of the interfacial heat transfer coefficient in porous media employing numerical simulations. *International Journal of Heat and Mass Transfer*, 60:406-412, 2013.
- Williams, P.T. and Baker, A.J., Numerical simulations of laminar flow over a 3D backward-facing step. *International Journal for Numerical Methods in Fluids*, 24:1159-1183, 1997.